https://doi.org/10.5194/essd-2020-398
Preprint. Discussion started: 8 March 2021

Earth System Science Data
Open Access Discussions

Patterns of nitrogen and phosphorus pools in terrestrial ecosystems in China

Yi-Wei Zhang[1#], Yanpei Guo[1#], Zhiyao Tang[1]*, Yuhao Feng[1], Xinrong Zhu[1], Wenting Xu[2], Yongfei Bai[2], Guoyi Zhou[3], Zongqiang Xie[2], Jingyun Fang[1]

[1]Institute of Ecology, College of Urban and Environmental Sciences and Key Laboratory for Earth Surface Processes of the Ministry of Education, Peking University, Beijing 100871

[2]State Key Laboratory of Vegetation and Environmental Change, Institute of Botany, Chinese Academy of Sciences, Beijing 100093

[3]Institute of Ecology, Jiangsu Key Laboratory of Agricultural Meteorology, Nanjing University of Information Science & Technology, Nanjing 210044, China

[#]Equal contribution

Corresponding author:
Zhiyao Tang, Ph.D.
E-mail: zytang@urban.pku.edu.cn
Tel/Fax: +86-10-6275-4039

https://doi.org/10.5194/essd-2020-398
Preprint. Discussion started: 8 March 2021

Abstract

Recent increases in atmospheric carbon dioxide (CO_2) and temperature relieve the limitation of these two on terrestrial ecosystem productivity, while nutrient availability constrains the increasing plant photosynthesis more intensively. Nitrogen (N) and phosphorus (P) are critical for plant physiological activities and consequently regulates ecosystem productivity. Here, for the first time, we mapped N and P densities of leaves, woody stems, roots, litter and soil in forest, shrubland and grassland ecosystems across China, based on an intensive investigation in 4175 sites, covering species composition, biomass, and nutrient concentrations of different tissues of living plants, litter and soil. Forest, shrubland and grassland ecosystems in China stored 7665.62×10^6 Mg N, with 7434.53×10^6 Mg (96.99%) fixed in soil (to a depth of one metre), and 32.39×10^6 Mg (0.42%), 59.57×10^6 Mg (0.78%), 124.21×10^6 Mg (1.62%) and 14.92×10^6 Mg (0.19%) in leaves, stems, roots and litter, respectively. The forest, shrubland and grassland ecosystems in China stored 3852.66×10^6 Mg P, with 3821.64×10^6 Mg (99.19%) fixed in soil (to a depth of one metre), and 3.36×10^6 Mg (0.09%), 14.06×10^6 Mg (0.36%), 11.47×10^6 Mg (0.30%) and 2.14×10^6 Mg (0.06%) in leaves, stems, roots and litter, respectively. Our estimation showed that N pools were low in northern China except Changbai Mountains, Mount Tianshan and Mount Alta, while relatively higher values existed in eastern Qinghai-Tibetan Plateau and Yunnan. P densities in plant organs were higher towards the south and east part of China, while soil P density was higher towards the north and west part of China. The estimated N and P density datasets, "Patterns of nitrogen and phosphorus pools in terrestrial ecosystems in China" (the pre-publication sharing link: https://datadryad.org/stash/share/78EBjhBqNoam2jOSoO1AXvbZtgIpCTi9eT-eGE7wyOk), are available from the Dryad Digital Repository (Zhang et al., 2020). These patterns of N and

https://doi.org/10.5194/essd-2020-398
Preprint. Discussion started: 8 March 2021

P densities could potentially improve existing earth system models and large-scale researches on ecosystem nutrients.

Key words: climate; nitrogen pools; phosphorus pools; nutrient limitation; spatial distribution

https://doi.org/10.5194/essd-2020-398
Preprint. Discussion started: 8 March 2021

1 Introduction

Nitrogen (N) and phosphorus (P) play fundamental roles in plant physiological activities and functioning, such as photosynthesis, resource utilization and reproductive behaviours (Fernández-Martínez et al., 2019; Lovelock et al., 2004; Raaimakers et al., 1995), ultimately regulating plant growth and carbon (C) sequestration efficiency (Terrer et al., 2019). Under the background of global warming, the limiting factors for the plant growth, such as carbon dioxide (CO_2) and temperature, are becoming less restrictive for terrestrial ecosystem productivity (Norby et al., 2009), while nutrient availability tends to constrain the increasing plant photosynthesis more intensively (Cleveland et al., 2013; Du et al., 2020). As the key nutrients for plant growth, N and P independently or together limit biomass production (Elser et al., 2007; Finzi et al., 2007). N influence CO_2 assimilation in various ways (Vitousek and Howarth, 1991). For example, N is a critical element in chlorophyll (Field, 1983), and plant metabolic rates are also regulated by N content (Elser et al., 2010). P is crucial in RNA and DNA construction, and its content is associated with water uptake and transport (Carvajal et al., 1996; Cheeseman and Lovelock, 2004) as well as energy transfer and exchange (Achat et al., 2009). P shortage could lower photosynthetic C-assimilation rates (Lovelock et al., 2006).

In spite of the key importance of N and P for plants, knowledge on the patterns of their storage in terrestrial ecosystems are limited. With additional CO_2 entering atmosphere, more N could be allotted to plant growth and soil organic matter (SOM) accumulation, which may lead to less available mineral N for plant uptake (Luo et al., 2004). Direct and indirect evidences show that N limits productivity in temperate and boreal areas (Bonan, 1990; Miller, 1981; Vitousek, 1982). P originates from bedrock weathering and litter decomposition in terrestrial ecosystems, and it experiences long-term biogeochemical processes before available to plants

https://doi.org/10.5194/essd-2020-398
Preprint. Discussion started: 8 March 2021

(Föllmi, 1996), which consequently makes P a more predominant limiting factor to ecosystem productivity (Reed et al., 2015). Additionally, P decomposition rates are constrained by limited soil labile P storage, especially in tropical forests where soil P limitation is extreme (Fisher et al., 2012).

Ecosystem models based on Amazon forest free air CO_2 enrichment (FACE) experiments consistently showed that biomass C positively responded to simulated elevated CO_2, but the models incorporating N and P availability showed lower plant growth than those not (Wieder et al., 2015). Moreover, a recent study suggested that the inclusion of N and P availability into the earth system models (ESMs) remarkably improved the estimation accuracy of C cycles over previous models (Fleischer et al., 2019). Hence, understanding and predicting the patterns and mechanisms of global C dynamics require well characterizing of N and P conditions.

N and P pools in ecosystems consist of several components that cast different influences on ecosystem C storages and fluxes. For example, N and P in plants directly affect C sequestration (Thomas et al., 2010), but their activities differ among organs (Elser et al., 2003; Parks et al., 2000); the soil pools are the source of plant nutrition; and the litter pools act as a transit link that returns nutrients from plants to soil (McGrath et al., 2000). Thus, an accurate estimation of ecosystem N and P pools involves calculating specific nutrient densities in all these components.

Terrestrial ecosystems in China play a considerable part in the continental and global C cycles. Satellite data verified that China contributed to a 1/4 of global net increase in leaf area from 2000 to 2017 (Chen et al., 2019). The total C pool in terrestrial ecosystems in China is 79.2 Pg C, and this number is still growing because of the nationwide ecological restoration constructions, which accounted for 56% of the total C sequestration in the restoration area in

https://doi.org/10.5194/essd-2020-398
Preprint. Discussion started: 8 March 2021

China from 2001 to 2010 (Lu et al., 2018). N and P limitations are ubiquitous in natural ecosystems in China (Du et al., 2020). Understanding the distribution and allocation of N and P in ecosystems is of great significance for a precise projection of C cycle in China. Although there are a few studies on the spatial patterns of soil nutrient storages in China (Shangguan et al., 2013; Yang et al., 2007; Zhang et al., 2005), a thorough study on the distribution of N and P pools of the whole ecosystems is still lacking, as vegetation (living or dead biomass) composes the most active part of the nutrient stocks.

To fill this knowledge gap, here we identified N and P density patterns in China based on an intensive field investigation, covering all components of the entire ecosystem, including different plant organs, litter and soil. The present study aims to provide a high-resolution map of nutrient densities in different ecosystem components and to answer the following questions.

1) How much N and P are stored in different components, i.e., leaf, stem, root, litter and soil, of terrestrial ecosystems in China?

2) How do different components of N and P pools spatially distribute in China?

2 Material and methods

2.1 Field sampling and nutrient density calculation

Forest, shrublands and grasslands constitute major vegetation type groups in China. Focusing primarily on these three groups, a nationwide, methodologically consistent field investigation was conducted in June and September, 2011-2015.

In total, 4175 sites, including 2385 forest, 1069 shrubland and 721 grassland sites, were investigated. At each site, one 20 × 50 m^2 plot was set for forests, three replicated 5 × 5 m^2 plots were set for shrublands, and ten 1 × 1 m^2 plots were established for grasslands. Species composition and abundance were investigated in plots. Height (for trees, shrubs and herbs),

https://doi.org/10.5194/essd-2020-398
Preprint. Discussion started: 8 March 2021

diameter at breast height (DBH, at height 130 cm) (for trees), basal diameter (for shrubs) and crown width (for shrubs and herbs) were measured for all plant individuals in the plots (Tang et al., 2018a).

Leaves, stems (woody stems) and roots (without distinguishing coarse and fine roots) were sampled for the five top dominant tree and shrub species, and above- and belowground parts were sampled for dominant herb species. Soil was sampled at the depths of 0–10, 10–20, 20–30, 30–50, and 50–100 cm with at least five replications per site to measure nutrient concentrations and bulk density after removing roots and gravels. Litter was sampled in at least three 1 × 1 m^2 quadrats per site (for detailed survey protocol, see Tang et al., 2018a).

All samples were transported to laboratory, dried and measured. N concentrations of all samples were measured by a C/N analyzer (PE-2400 II; Perkin-Elmer, Boston, USA), while P concentrations were measured using the molybdate/ascorbic acid method after H_2SO_4-H_2O_2 digestion. For the three organs, the community-level N or P density was the cumulative sum of the products of the corresponding biomass density (i.e. biomass per area, Mg ha^{-1}) and community-level concentrations for each co-occurring species. For detailed calculation of species biomass and community-level concentrations in each site, please referred to Tang et al (2018b).

$$N(P) = \sum B_i \times \theta_i \quad (1)$$

$N(P)$ represents the community-level N or P density (Mg ha^{-1}); B_i is the biomass density of a specific organ of the i^{th} plant species in one site, where the plant organ biomass was estimated by allometric equations or harvesting; θ_i represents the N or P concentration (g kg^{-1}) of the same organ of the i^{th} plant species in that site. Allometric equation methods were adapted to trees and some shrubs (tree-like shrubs and xeric shrubs) for biomass estimation,

https://doi.org/10.5194/essd-2020-398
Preprint. Discussion started: 8 March 2021

while the biomass of grass-like shrubs and herbs were obtained by direct harvesting. Litter N or P density was litter biomass density (by harvesting) multiplied by litter N or P concentration of each sampling site. The soil N or P density was calculated to a depth of one metre. Soil N or P concentration and bulk density were measured at different depths (0–10, 10–20, 20–30, 30–50, and 50–100 cm) to determine the community-level soil N or P density using Equation (2):

$$SOND(SOPD) = \sum(1 - \delta_i) \times \rho_i \times C_i \times T_i/10 \quad (2)$$

where $SOND(SOPD)$ is the total N or P density of the soil (Mg ha^{-1}) in the i^{th} layer (0-10, 10-20, 20-30, 30-50 and 50-100 cm), δ_i is the volume percentage of gravel with a diameter > 2mm, ρ_i is the bulk density (g cm^{-3}), C_i is the soil N or P concentration (g kg^{-1}), and T_i is the depth (cm) of the i^{th} layer. For detailed calculations of species biomass and community-level concentrations at each site, please refer to previous studies (Tang et al., 2018a, 2018b).

2.2 Climatic and vegetation data

The daily meteorological observation data from 2,400 meteorological stations across China were averaged over the 2011-2015 period to generate a spatial interpolation dataset of mean annual temperature (MAT) and precipitation (MAP), using a smooth spline function (McVicar et al., 2007) , with a spatial resolution of 1 km. MAT and MAP of each site were extracted from this dataset.

Elevation was extracted from GTOPO30 with a spatial resolution of 30 arc-seconds (http://edc.usgs.gov/products/elevation/gtopo30/gtopo30.html). The mean enhanced vegetation index (EVI) from June to September during the 2011–2015 period was calculated based on MOD13A3 data with a resolution of 1 km (https://modis.gsfc.nasa.gov/).

Based on the level II vegetation classification of ChinaCover (Land Cover Atlas of the

https://doi.org/10.5194/essd-2020-398
Preprint. Discussion started: 8 March 2021

People's Republic of China Editorial Board, 2017), we classified the vegetation type groups into the following 13 Vegetation types: five forest types, i.e., evergreen broadleaf forests, deciduous broadleaf forests, evergreen needle-leaf forests, deciduous needle-leaf forests, broadleaf and needle-leaf mixed forests; four shrubland types, i.e., evergreen broadleaf shrublands, deciduous broadleaf shrublands, evergreen needle-leaf shrublands, and sparse shrublands; and four grassland types, i.e., meadows, steppes, tussocks, and sparse grasslands.

2.3 Prediction the nationwide nutrient pools and distribution patterns

We used back-propagation artificial neural network for nutrient density spatial interpolating. The input layer contained MAT, MAP, longitude, latitude, elevation, EVI and vegetation types (as dummy variables). We established one artificial neural network for N and P in five components, respectively. The observation data were randomly grouped into two subsets, 90% data for training and the other 10% for validation. When building the artificial network, we used one and two layers, one to 20 hidden neurons per layer, respectively, to find out a model configuration with the best predicting ability. The training and testing process were repeated 100 times for each configuration. The best predicting model was selected according to the minimal mean root mean square error (RMSE). Then the chosen model was used to predict the nationwide nutrient distribution in corresponding component for 100 times to obtain the average conditions.

When modelling the nutrient densities in woody stems, we excluded the four grassland types. The vegetation N or P density was the sum of all plant organs, and the ecosystem N or P density was the sum of all components.

All densities were log-transformed based on *e*, and explanatory variables were transformed

https://doi.org/10.5194/essd-2020-398
Preprint. Discussion started: 8 March 2021

using the following equation to ensure they were in the same range before modelling.

$$x_i' = \frac{x_i - min(x)}{max(x) - min(x)} \quad (3)$$

where x_i means the i^{th} value of the environmental variables x, and max(x) and min(x) represent the maximum and minimum values of x, respectively.

The N and P pools in 13 Vegetation types were estimated, respectively. The N and P pools were calculated from the predicted nationwide densities. The predicted N and P densities were in 1 km spatial resolution, so the nutrient stock is the density multiply the grid area (1 km^2) for each grid. The nutrient pools of a given vegetation type equals the sum of stocks of the grids belonging to that type.

2.4 Data Model uncertainty and validation

To evaluate the model performance, we calculated the linear relationship between the observed validation data (10% of the dataset by random sampling) and predicted data that was estimated based on training data (90% of the dataset by random sampling) for 100 times with the selected models for every component. The R^2, slopes and intercepts of these relationships were estimated using standard major axis regression. We also mapped the standard deviations (SDs) of the 100-time predictions of each component to show the uncertainty of our results in different regions.

All statistical analyses were performed using R 3.6.1 (R Core Team, 2019), artificial networks were built using *neuralnet* package (Günther and Fritsch, 2010), and standard major axis regression was conducted using *smatr* package (Warton et al., 2012).

3 Data accessibility

https://doi.org/10.5194/essd-2020-398
Preprint. Discussion started: 8 March 2021

The datasets of N and P densities of different ecosystem components, " Patterns of nitrogen and phosphorus pools in terrestrial ecosystems in China", are available from the Dryad Digital Repository (the pre-publication sharing link: https://datadryad.org/stash/share/78EBjhBqNoam2jOSoO1AXvbZtgIpCTi9eT-eGE7wyOk) (Zhang et al., 2020).

4 Results

4.1 Site average allocation of nutrient among ecosystem components

The site averaged N and P densities varied among forests, shrublands and grasslands and among different tissues (Fig. 1 & 2) according to the measured plot data. In average, leaves and woody stems in the forests stored more N than those in the shrublands (11 ± 10 (mean ± SD) × 10^{-2} Mg N ha^{-1} vs. 3.2 ± 10 × 10^{-2} Mg N $ha^{-1}$for leaves, and 260 ± 340 × 10^{-3} Mg N ha^{-1} vs. 5.8 ± 11 × 10^{-3} Mg N ha^{-1} for woody stems). Similarly, P densities were higher in the forests leaves and woody stems than those in the shrublands (12 ± 13 × 10^{-3} Mg P ha^{-1} vs. 2.9 ± 6.1 × 10^{-3} Mg P ha^{-1} for leaves and 52 ± 110× 10^{-3} Mg P ha^{-1} vs. 4.4 ± 11 × 10^{-3} Mg P ha^{-1} for woody stems). than those in shrublands (3.2 ± 10 × 10^{-2} Mg N ha^{-1} and 2.9 ± 6.1 × 10^{-3} Mg P ha^{-1} for leaves; 5.8 ± 11 × 10^{-3} Mg N ha^{-1} and 4.4 ± 11 × 10^{-3} Mg P ha^{-1} for woody stems) and grasslands (2.7 ± 2.4 × 10^{-2} Mg N ha^{-1} and 2.7 ± 2.9 × 10^{-3} Mg P ha^{-1} for leaves). However, the root N and P densities in forests (1.3 ± 1.6 × 10^{-1} Mg N ha^{-1} and 1.8 ± 2.8 × 10^{-2} Mg P ha^{-1}) and grasslands (1.9 ± 1.7 × 10^{-1} Mg N ha^{-1} and 1.5 ± 1.6 × 10^{-2} Mg P ha^{-1}) were remarkably higher than in shrublands (6.5 ± 11 × 10^{-2} Mg N ha^{-1} and 6.1 ± 9.9 × 10^{-3} Mg P ha^{-1}).

The site-averaged litter N densities in forests, shrublands and grasslands were 6.3 ± 8.1 × 10^{-2} Mg N ha^{-1}, 3.2 ± 4.1 × 10^{-2} Mg N ha^{-1} and 5.5 ± 9.3 × 10^{-3} Mg N ha^{-1}, respectively. The

https://doi.org/10.5194/essd-2020-398
Preprint. Discussion started: 8 March 2021

site-averaged litter P densities in forests, shrublands and grasslands were 5.3 ± 9.9× 10^{-3} Mg P ha^{-1}, 2.2 ± 2.9× 10^{-3} Mg P ha^{-1} and 4.14 ± 7.1 × 10^{-4} Mg P ha^{-1}, respectively.

The site-averaged soil N densities in forests, shrublands and grasslands were 11.2 ± 9.2 Mg N ha^{-1}, 9.4 ± 7.8 Mg N ha^{-1} and 9.9 ± 8.9 Mg N ha^{-1}, respectively. The site-averaged soil P densities were 4.6 ± 4.2 Mg P ha^{-1} in forest, 4.0 ± 3.0 Mg P ha^{-1} in shrublands and 4.1 ± 2.7 Mg P ha^{-1} in grasslands.

Both belowground vegetation N and P densities were higher than aboveground in shrublands and grasslands. By contrast, this condition was reversed in forests (Fig. 3). Among various forest types, deciduous needle-leaf forests held the highest aboveground N and P densities. Evergreen needle-leaf forests held the lowest vegetation N density and evergreen broadleaf forests owned lowest P density. For grassland types, the density allocation varied markedly. Meadows and steppes held higher N and P densities in belowground biomass than tussocks and sparse grasslands, whereas these four grasslands types had relatively approximate nutrient densities in aboveground biomass. Shrublands possessed the lowest vegetation N and P densities among three vegetation groups. Sparse shrublands owned the lowest vegetation nutrient densities and soil N density but the highest soil P density among four shrubland types.

4.2 Mapping of N and P densities in China's terrestrial ecosystems

All models of the N and P densities of different components performed well (Fig. 4), especially those for the woody stems (R^2 = 0.81 and 0.69 for N and P densities, respectively) and litter (R^2=0.66 and 0.62 for N and P densities, respectively). SDs of N and P densities were relatively higher in western and northeastern China, with values > 5 (Fig. 5k–t). For example, the predictions of litter N (Fig. 5q) and P (Fig. 5r) showed larger SDs in western Xinjiang and

https://doi.org/10.5194/essd-2020-398
Preprint. Discussion started: 8 March 2021

Tibet.

The leaf N density was high in southern and eastern China, but low in northern and western China. It was especially high in the Changbai Mountains, the southern Tibet and the southeast coastal areas (Fig. 5), with a density of >0.1 Mg N ha^{-1}. In comparison, it was low in the northern Xinjiang and northern Inner Mongolia (< 0.01 Mg N ha^{-1}). The woody stem and litter N densities showed the similar patterns to those of the leaves, whereas that in roots was high in the Mount Tianshan, Mount Alta, Qinghai-Tibetan Plateau, northeastern mountainous area and the Inner Mongolia steppe (Fig. 5). The vegetation N density was relatively high in eastern China, Qinghai-Tibetan Plateau, Mount Tianshan and Mount Alta, ranging from 0.5 to 2.5 Mg N ha^{-1}. The soil and ecosystem N densities were low in northern China except the Changbai Mountains, Mount Tianshan and Mount Alta, but high in the eastern Qinghai-Tibetan Plateau and the Yunnan Province (Fig. 6).

The P densities in leaves, woody stems, roots and litter showed similar patterns to the N densities in the corresponding components, respectively. However, soil and ecosystem P densities were high in western and northern China but low in eastern and southern China, but low at high altitudes in the Qinghai-Tibetan Plateau (Fig. 5 & 6).

4.3 N and P pools in China's terrestrial ecosystems

In total, the terrestrial ecosystems in China stored 7665.62 × 10^6 Mg N, with 2632.80 × 10^6 Mg N, 830.24 × 10^6 Mg N and 4202.58 × 10^6 Mg N stored in the forests, shrublands and grasslands, respectively (Table 1). Vegetation, litter and soil stored 216.17 × 10^6 Mg N (2.82%), 14.92 × 10^6 Mg N (0.19%) and 7434.53 × 10^6 Mg N (96.99%), respectively.

China's terrestrial ecosystems stored 3852.66 × 10^6 Mg P, with 1037.34 × 10^6 Mg P, 361.62

× 10^6 Mg P and 2453.70 × 10^6 Mg P stored in the forest, shrublands and grasslands, respectively. Vegetation, litter and soil accounted for 28.88 × 10^6 Mg P (0.75%), 2.14 × 10^6 Mg P (0.06%) and 3821.64 × 10^6 Mg P (99.19%), respectively.

Meanwhile, N and P stocks among plant organs showed different allocation patterns (Table 2). Compared with the other two vegetation type groups, forests allocated the majority of N and P to the stem pool (59.29× 10^6 Mg N and 13.81× 10^6 Mg P), followed by the root pool (28.55× 10^6 Mg N and 5.53× 10^6 Mg P) and leaf pool (23.84× 10^6 Mg N and 2.49× 10^6 Mg P). However, the root pools in shrublands and grasslands held the most of N and P (4.44× 10^6 Mg N and 0.38× 10^6 Mg P for shrublands, and 91.22× 10^6 Mg N and 5.55× 10^6 Mg P for grasslands).

Among 4 grassland types, steppe had the largest N stock (1599.47× 10^6 Mg N), and sparse grasslands had the largest P stock (1578.83× 10^6 Mg P) taking the ecosystem as a whole. Deciduous broadleaf shrublands owned the largest N and P stocks considering the whole ecosystem (605.09× 10^6 Mg N and 211.15× 10^6 Mg P) as well as in vegetation (5.30× 10^6 Mg N and 0.58× 10^6 Mg P), compared with the other 3 shrubland types. The largest ecosystem N and P stocks across all 13 vegetation types appeared in evergreen needle-leaf forests (43.43× 10^6 Mg N and 8.37× 10^6 Mg).

5 Discussion

5.1 Performance and uncertainty of density models

The accuracy of the models varied among different components. Soil interpolation models showed poorest accuracy (R^2=0.38 for N and 0.27 for P) among these models, partly because that soil N and P were more stable than those in the plants and litters (Matamala et al., 2008) and that soil nutrient exchange and storage were largely controlled by geochemical and

https://doi.org/10.5194/essd-2020-398
Preprint. Discussion started: 8 March 2021

geophysical processes (Doetterl et al., 2015), which are not considered in our models. The models preformed best for the stem N and P, because woody stems occupied the most biomass in the forest and shrublands (stem biomass/vegetation biomass were 0.68 and 0.48 for forest and shrublands, respectively). Climate variables could affect vegetation growth and biomass accumulation, and the variation in stem biomass could be the most direct reflection (Jozsa and Powell, 1987; Kirilenko and Sedjo, 2007; Poudel et al., 2011).

The predicted SDs were relatively higher in high-latitudes and high-altitudes, such as the northeastern mountainous area and the Qinghai-Tibet Plateau, probably because of the lower sampling density. Meanwhile, the temperature in these regions was about the lower limit of the temperature range in our dataset, which could consequently lead to the weaker validity of the prediction results in such cold regions.

5.2 Potential driving factors of the N and P densities in various components

The distribution and allocation of N and P pools in ecosystems were largely determined by vegetation types and climate. The difference in the spatial patterns of nutrient pools could reflect the spatial variation in local vegetation. For example, it is obvious that the regions covered by forests tend to have higher the aboveground nutrient densities than those covered by other types, while the regions covered by sparse shrublands tend to have the lowest nutrient densities (Fig. 3). Despite its decisive influences on vegetation types, climate also impacts greatly on the nutrient utilization strategies of vegetation (Kirilenko and Sedjo, 2007; Poudel et al., 2011). For example, in southeastern China with higher precipitation and temperature, forests tend to allot more nutrient to organs related to growth, for example, leaves that perform photosynthesis and stems that related to resource transport and light competition (Zhang et al.,

https://doi.org/10.5194/essd-2020-398
Preprint. Discussion started: 8 March 2021

2018). Heat and water are usually limited in the plateau and desert regions in western China, where shrublands and grasslands are dominant vegetation type groups. More nutrients are allocated to root systems by dominant plants in such stressful habitats to acquire resources from soil (Eziz et al., 2017; Kramer-Walter and Laughlin, 2017). Soil nutrient densities were relatively larger in the plateau and mountainous area in western China, possibly because of the lower rates of decomposition, mineralization, and nutrient uptake as well as less leaching loss in high-altitude regions (Bonito et al., 2003; Vincent et al., 2014). However, the distribution patterns of soil nutrient densities in eastern China were generally consistent with the Soil Substrate Age hypothesis that the younger and less-leached soil in temperate regions tend to be more N limited but less P limited than the elder and more-leached soil in tropical and subtropical regions (Reich and Oleksyn, 2004; Vitousek et al., 2010).

5.3 Potential applications of the data

Atmospheric CO_2 enrichment trend was undoubtable, but how this procedure will develop is still unclear (Fatichi et al., 2019). A number of previous studies proved that global carbon cycle models would produce remarkable bias if overlooking the coupled nutrient cycle (Fleischer et al., 2019; Hungate et al., 2003; Thornton et al., 2007). However, high-resolution and accurate ecosystem nutrient datasets were unattainable and hard to be modeled without enormous field investigation basis. This study relied on nationwide field survey data, providing comprehensive N and P density datasets of different ecosystem components. Based on the present dataset, enhancement could be made in various ecosystem research aspects.

First and foremost, the dataset could facilitate the improvement in the prediction of large-scale terrestrial C budget, thereby to better understand patterns and mechanisms of C cycle as well as the future trend of climate change (Le Quéré et al., 2018). Numerous projections of future C sequestration overestimated the amount of C fixed by vegetation due to the neglect of nutrient limitation (Cooper et al., 2002; Cramer et al., 2001). Global C cycling models coupled with nutrient cycle could make more accurate predictions of carbon dynamics. Moreover, our dataset illustrated N and P densities of major ecosystem components and vegetation types at a high spatial resolution for the first time, which could help identify C and nutrient allocation patterns from the tissue level to the community level, especially for vegetation organs which still lack large-scale nutrient datasets.

In addition, large-scale N and P pool spatial patterns could provide the data references for the vegetation researches using remote sensing (Jetz et al., 2016). Vegetation nutrient densities was important traits but hard to be extracted and detected remotely. With the development of hyperspectral remote sensing technology and theory of spectral diversity, foliar nutrient traits can be successfully predicted (Skidmore et al., 2010; Wang et al., 2019). However, previous studies still focused on finer-scale patterns and were constrained by the lack of large-scale field datasets for uncertainties assessment (Singh et al., 2015). Our nationwide nutrient dataset offers an opportunity to enlarge the generality of remote-sensing models and algorithms at large scales.

Funding

This work was funded by the National Key Research and Development Project (2019YFA0606602), the National Natural Science Foundation of China (32025025, 31770489, 31988102) and the Strategic Priority Research Programme of the Chinese Academy of Sciences (XDA27010102, XDA05050000).

Author Contributions

https://doi.org/10.5194/essd-2020-398
Preprint. Discussion started: 8 March 2021

Z.T. designed the research. Y.W.Z, Y.G., Y.F., and X.Z. analysed the data. W.X., Y.B., G.Z., Z.X. and Z.T. organized the field investigation. Y.W.Z, Y.G., Z.T. wrote the manuscript and all authors contributed substantially to revisions.

Competing interests

The authors declare no competing interests.

https://doi.org/10.5194/essd-2020-398
Preprint. Discussion started: 8 March 2021

Reference

Achat, D. L., Bakker, M. R. and Morel, C.: Process-based assessment of phosphorus availability in a low phosphorus sorbing forest soil using isotopic dilution methods., Soil Sci. Soc. Am. J., 73(6), 2131–2142, 2009.

Bonan, G. B.: Carbon and nitrogen cycling in North American boreal forests, Biogeochemistry, 10(1), 1–28, doi:10.1007/BF00000889, 1990.

Bonito, G. M., Coleman, D. C., Haines, B. L. and Cabrera, M. L.: Can nitrogen budgets explain differences in soil nitrogen mineralization rates of forest stands along an elevation gradient?, Forest Ecology and Management, 176(1), 563–574, doi:10.1016/S0378-1127(02)00234-7, 2003.

Carvajal, M., Cooke, D. T. and Clarkson, D. T.: Responses of wheat plants to nutrient deprivation may involve the regulation of water-channel function, Planta, 199(3), 372–381, doi:10.1007/BF00195729, 1996.

Cheeseman, J. M. and Lovelock, C. E.: Photosynthetic characteristics of dwarf and fringe Rhizophora mangle L. in a Belizean mangrove, Plant Cell Environ., 27(6), 769–780, doi:10.1111/j.1365-3040.2004.01181.x, 2004.

Chen, C., Park, T., Wang, X., Piao, S., Xu, B., Chaturvedi, R. K., Fuchs, R., Brovkin, V., Ciais, P., Fensholt, R., Tømmervik, H., Bala, G., Zhu, Z., Nemani, R. R. and Myneni, R. B.: China and India lead in greening of the world through land-use management, Nat. Sustain., 2(2), 122–129, doi:10.1038/s41893-019-0220-7, 2019.

Cleveland, C. C., Houlton, B. Z., Smith, W. K., Marklein, A. R., Reed, S. C., Parton, W., Grosso, S. J. D. and Running, S. W.: Patterns of new versus recycled primary production in the terrestrial biosphere, Proc. Natl. Acad. Sci. U. S. A., 110(31), 12733–12737, doi:10.1073/pnas.1302768110, 2013.

Cooper, R. N., Houghton, J. T., McCarthy, J. J. and Metz, B.: Climate Change 2001: The Scientific Basis, Cambridge University Press, Cambridge, UK. [online] Available from: https://www.jstor.org/stable/10.2307/20033020?origin=crossref (Accessed 7 December 2019), 2002.

Cramer, W., Bondeau, A., Woodward, F. I., Prentice, I. C., Betts, R. A., Brovkin, V., Cox, P. M., Fisher, V., Foley, J. A., Friend, A. D., Kucharik, C., Lomas, M. R., Ramankutty, N., Sitch, S., Smith, B., White,

A. and Young-Molling, C.: Global response of terrestrial ecosystem structure and function to CO_2 and climate change: results from six dynamic global vegetation models, Glob. Change Biol., 7(4), 357–373, doi:10.1046/j.1365-2486.2001.00383.x, 2001.

Doetterl, S., Stevens, A., Six, J., Merckx, R., Van Oost, K., Casanova Pinto, M., Casanova-Katny, A., Muñoz, C., Boudin, M., Zagal Venegas, E. and Boeckx, P.: Soil carbon storage controlled by interactions between geochemistry and climate, Nat. Geosci., 8(10), 780–783, doi:10.1038/ngeo2516, 2015.

Du, E., Terrer, C., Pellegrini, A. F. A., Ahlström, A., van Lissa, C. J., Zhao, X., Xia, N., Wu, X. and Jackson, R. B.: Global patterns of terrestrial nitrogen and phosphorus limitation, Nature Geoscience, 13(3), 221–226, doi:10.1038/s41561-019-0530-4, 2020.

Elser, J. J., Acharya, K., Kyle, M., Cotner, J., Makino, W., Markow, T., Watts, T., Hobbie, S., Fagan, W., Schade, J., Hood, J. and Sterner, R. W.: Growth rate–stoichiometry couplings in diverse biota, Ecol. Lett., 6(10), 936–943, doi:10.1046/j.1461-0248.2003.00518.x, 2003.

Elser, J. J., Bracken, M. E. S., Cleland, E. E., Gruner, D. S., Harpole, W. S., Hillebrand, H., Ngai, J. T., Seabloom, E. W., Shurin, J. B. and Smith, J. E.: Global analysis of nitrogen and phosphorus limitation of primary producers in freshwater, marine and terrestrial ecosystems, Ecol. Lett., 10(12), 1135–1142, doi:10.1111/j.1461-0248.2007.01113.x, 2007.

Elser, J. J., Fagan, W. F., Kerkhoff, A. J., Swenson, N. G. and Enquist, B. J.: Biological stoichiometry of plant production: metabolism, scaling and ecological response to global change: Tansley review, New Phytologist, 186(3), 593–608, doi:10.1111/j.1469-8137.2010.03214.x, 2010.

Fernández-Martínez, M., Pearse, I., Sardans, J., Sayol, F., Koenig, W. D., LaMontagne, J. M., Bogdziewicz, M., Collalti, A., Hacket-Pain, A., Vacchiano, G., Espelta, J. M., Peñuelas, J. and Janssens, I. A.: Nutrient scarcity as a selective pressure for mast seeding, Nat. Plants, 5(12), 1222–1228, doi:10.1038/s41477-019-0549-y, 2019.

Field, C.: Allocating leaf nitrogen for the maximization of carbon gain: Leaf age as a control on the allocation program, Oecologia, 56(2), 341–347, doi:10.1007/BF00379710, 1983.

Finzi, A. C., Norby, R. J., Calfapietra, C., Gallet-Budynek, A., Gielen, B., Holmes, W. E., Hoosbeek, M. R., Iversen, C. M., Jackson, R. B., Kubiske, M. E., Ledford, J., Liberloo, M., Oren, R., Polle, A., Pritchard, S., Zak, D. R., Schlesinger, W. H. and Ceulemans, R.: Increases in nitrogen uptake rather than nitrogen-use efficiency support higher rates of temperate forest productivity under elevated CO2, Proc. Natl. Acad. Sci. U. S. A., 104(35), 14014–14019, doi:10.1073/pnas.0706518104, 2007.

Fisher, J. B., Badgley, G. and Blyth, E.: Global nutrient limitation in terrestrial vegetation, Glob. Biogeochem. Cycle, 26(3), GB3007, doi:10.1029/2011GB004252, 2012.

Fleischer, K., Rammig, A., De Kauwe, M. G., Walker, A. P., Domingues, T. F., Fuchslueger, L., Garcia, S., Goll, D. S., Grandis, A., Jiang, M., Haverd, V., Hofhansl, F., Holm, J. A., Kruijt, B., Leung, F., Medlyn, B. E., Mercado, L. M., Norby, R. J., Pak, B., von Randow, C., Quesada, C. A., Schaap, K. J., Valverde-Barrantes, O. J., Wang, Y.-P., Yang, X., Zaehle, S., Zhu, Q. and Lapola, D. M.: Amazon forest response to CO2 fertilization dependent on plant phosphorus acquisition, Nat. Geosci., 12(9), 736–741, doi:10.1038/s41561-019-0404-9, 2019.

Föllmi, K. B.: The phosphorus cycle, phosphogenesis and marine phosphate-rich deposits, Earth-Sci. Rev., 40(1), 55–124, doi:10.1016/0012-8252(95)00049-6, 1996.

Günther, F. and Fritsch, S.: neuralnet: Training of neural networks, The R journal, 2(1), 30–38, doi:10.32614/RJ-2010-006, 2010.

Hungate, B. A., Dukes, J. S., Shaw, M. R., Luo, Y. and Field, C. B.: Nitrogen and climate change, Science, 302(5650), 1512–1513, doi:10.1126/science.1091390, 2003.

Jetz, W., Cavender-Bares, J., Pavlick, R., Schimel, D., Davis, F. W., Asner, G. P., Guralnick, R., Kattge, J., Latimer, A. M., Moorcroft, P., Schaepman, M. E., Schildhauer, M. P., Schneider, F. D., Schrodt, F., Stahl, U. and Ustin, S. L.: Monitoring plant functional diversity from space, Nat. Plants, 2(3), 16024, doi:10.1038/nplants.2016.24, 2016.

Jozsa, L. A. and Powell, J. M.: Some climatic aspects of biomass productivity of white spruce stem wood, Canadian Journal of Forest Research, 17(9), 1075–1079, doi:10.1139/x87-165, 1987.

Kirilenko, A. P. and Sedjo, R. A.: Climate change impacts on forestry, Proc. Natl. Acad. Sci. U. S. A., 104(50), 19697–19702, doi:10.1073/pnas.0701424104, 2007.

Land Cover Atlas of the People's Republic of China Editorial Board: Land Cover Atlas of the People's Republic of China (1:1000000), China Map Publishing House, Beijing., 2017.

https://doi.org/10.5194/essd-2020-398
Preprint. Discussion started: 8 March 2021

Le Quéré, C., Andrew, R. M., Friedlingstein, P., Sitch, S., Pongratz, J., Manning, A. C., Korsbakken, J. I., Peters, G. P., Canadell, J. G., Jackson, R. B., Boden, T. A., Tans, P. P., Andrews, O. D., Arora, V. K., Bakker, D. C. E., Barbero, L., Becker, M., Betts, R. A., Bopp, L., Chevallier, F., Chini, L. P., Ciais, P., Cosca, C. E., Cross, J., Currie, K., Gasser, T., Harris, I., Hauck, J., Haverd, V., Houghton, R. A., Hunt, C. W., Hurtt, G., Ilyina, T., Jain, A. K., Kato, E., Kautz, M., Keeling, R. F., Klein Goldewijk, K., Körtzinger, A., Landschützer, P., Lefèvre, N., Lenton, A., Lienert, S., Lima, I., Lombardozzi, D., Metzl, N., Millero, F., Monteiro, P. M. S., Munro, D. R., Nabel, J. E. M. S., Nakaoka, S., Nojiri, Y., Padin, X. A., Peregon, A., Pfeil, B., Pierrot, D., Poulter, B., Rehder, G., Reimer, J., Rödenbeck, C., Schwinger, J., Séférian, R., Skjelvan, I., Stocker, B. D., Tian, H., Tilbrook, B., Tubiello, F. N., van der Laan-Luijkx, I. T., van der Werf, G. R., van Heuven, S., Viovy, N., Vuichard, N., Walker, A. P., Watson, A. J., Wiltshire, A. J., Zaehle, S. and Zhu, D.: Global carbon budget 2017, Earth Syst. Sci. Data, 10(1), 405–448, doi:10.5194/essd-10-405-2018, 2018.

Lovelock, C. E., Feller, I. C., Mckee, K. L., Engelbrecht, B. M. J. and Ball, M. C.: The effect of nutrient enrichment on growth, photosynthesis and hydraulic conductance of dwarf mangroves in Panama, Funct Ecology, 18(1), 25–33, doi:10.1046/j.0269-8463.2004.00805.x, 2004.

Lovelock, C. E., Feller, I. C., Ball, M. C., Engelbrecht, B. M. J. and Ewe, M. L.: Differences in plant function in phosphorus- and nitrogen-limited mangrove ecosystems, New Phytol., 172(3), 514–522, doi:10.1111/j.1469-8137.2006.01851.x, 2006.

Lu, F., Hu, H., Sun, W., Zhu, J., Liu, G., Zhou, W., Zhang, Q., Shi, P., Liu, X., Wu, X., Zhang, L., Wei, X., Dai, L., Zhang, K., Sun, Y., Xue, S., Zhang, W., Xiong, D., Deng, L., Liu, B., Zhou, L., Zhang, C., Zheng, X., Cao, J., Huang, Y., He, N., Zhou, G., Bai, Y., Xie, Z., Tang, Z., Wu, B., Fang, J., Liu, G. and Yu, G.: Effects of national ecological restoration projects on carbon sequestration in China from 2001 to 2010, Proc. Natl. Acad. Sci. U. S. A., 115(16), 4039–4044, doi:10.1073/pnas.1700294115, 2018.

Luo, Y., Su, B., Currie, W. S., Dukes, J. S., Finzi, A., Hartwig, U., Hungate, B., McMurtrie, R. E., Oren, R., Parton, W. J., Pataki, D. E., Shaw, R. M., Zak, D. R. and Field, C. B.: Progressive nitrogen limitation of ecosystem responses to rising atmospheric carbon dioxide, BioScience, 54(8), 731–739, doi:10.1641/0006-3568(2004)054[0731:PNLOER]2.0.CO;2, 2004.

Matamala, R., Jastrow, J. D., Miller, R. M. and Garten, C. T.: Temporal changes in C and N stocks of restored prairie: implications for C sequestration strategies, Ecol. Appl., 18(6), 1470–1488, doi:10.1890/07-1609.1, 2008.

McGrath, D. A., Comerford, N. B. and Duryea, M. L.: Litter dynamics and monthly fluctuations in soil phosphorus availability in an Amazonian agroforest, For. Ecol. Manage., 131(1), 167–181, doi:10.1016/S0378-1127(99)00207-8, 2000.

McVicar, T. R., Van Niel, T. G., Li, L., Hutchinson, M. F., Mu, X. and Liu, Z.: Spatially distributing monthly reference evapotranspiration and pan evaporation considering topographic influences, Journal of Hydrology, 338(3–4), 196–220, doi:10.1016/j.jhydrol.2007.02.018, 2007.

Miller, H. G.: Forest Fertilization: Some Guiding Concepts, Forestry, 54(2), 157–167, doi:10.1093/forestry/54.2.157, 1981.

Norby, R. J., Warren, J. M., Iversen, C. M., Garten, C. T., Medlyn, B. E. and McMurtrie, R. E.: 1 CO2 Enhancement of Forest Productivity Constrained by 2 Limited Nitrogen Availability, Nature Precedings, 15, 2009.

Parks, S. E., Haigh, A. M. and Cresswell, G. C.: Stem tissue phosphorus as an index of the phosphorus status of Banksia ericifolia L. f., Plant Soil, 227(1), 59–65, doi:10.1023/A:1026563926187, 2000.

Poudel, B. C., Sathre, R., Gustavsson, L., Bergh, J., Lundström, A. and Hyvönen, R.: Effects of climate change on biomass production and substitution in north-central Sweden, Biomass and Bioenergy, 35(10), 4340–4355, doi:10.1016/j.biombioe.2011.08.005, 2011.

Thomas, R. Q., Canham, C. D., Weathers, K. C. and Goodale, C. L.: Increased tree carbon storage in response to nitrogen deposition in the US, Nat. Geosci., 3(1), 13–17, doi:10.1038/ngeo721, 2010.

R Core Team: R: A language and environment for statistical computing, Vienna. [online] Available from: https://cran.r-project.org/, 2019.

Raaimakers, D., Boot, R. G. A., Dijkstra, P., Pot, S. and Pons, T.: Photosynthetic rates in relation to leaf phosphorus content in pioneer versus climax tropical rainforest trees, Oecologia, 102(1), 120–125, 1995.

Reed, S. C., Yang, X. and Thornton, P. E.: Incorporating phosphorus cycling into global modeling efforts: a worthwhile, tractable endeavor, New Phytol., 208(2), 324–329, doi:10.1111/nph.13521, 2015.

Reich, P. B. and Oleksyn, J.: Global patterns of plant leaf N and P in relation to temperature and latitude, Proc. Natl. Acad. Sci. U. S. A., 101(30), 11001–11006, doi:10.1073/pnas.0403588101, 2004.

Shangguan, W., Dai, Y., Liu, B., Zhu, A., Duan, Q., Wu, L., Ji, D., Ye, A., Yuan, H., Zhang, Q., Chen, D., Chen, M., Chu, J., Dou, Y., Guo, J., Li, H., Li, J., Liang, L., Liang, X., Liu, H., Liu, S., Miao, C. and Zhang, Y.: A China data set of soil properties for land surface modeling, J. Adv. Model. Earth Syst., 5(2), 212–224, doi:10.1002/jame.20026, 2013.

Singh, A., Serbin, S. P., McNeil, B. E., Kingdon, C. C. and Townsend, P. A.: Imaging spectroscopy algorithms for mapping canopy foliar chemical and morphological traits and their uncertainties, Ecological Applications, 25(8), 2180–2197, doi:10.1890/14-2098.1, 2015.

Skidmore, A. K., Ferwerda, J. G., Mutanga, O., Van Wieren, S. E., Peel, M., Grant, R. C., Prins, H. H. T., Balcik, F. B. and Venus, V.: Forage quality of savannas — simultaneously mapping foliar protein and polyphenols for trees and grass using hyperspectral imagery, Remote Sensing of Environment, 114(1), 64–72, doi:10.1016/j.rse.2009.08.010, 2010.

Tang, X., Zhao, X., Bai, Y., Tang, Z., Wang, W., Zhao, Y., Wan, H., Xie, Z., Shi, X., Wu, B., Wang, G., Yan, J., Ma, K., Du, S., Li, S., Han, S., Ma, Y., Hu, H., He, N., Yang, Y., Han, W., He, H., Yu, G., Fang, J. and Zhou, G.: Carbon pools in China's terrestrial ecosystems: New estimates based on an intensive field survey, Proc Natl Acad Sci USA, 115(16), 4021–4026, doi:10.1073/pnas.1700291115, 2018a.

Tang, Z., Xu, W., Zhou, G., Bai, Y., Li, J., Tang, X., Chen, D., Liu, Q., Ma, W., Xiong, G., He, H., He, N., Guo, Y., Guo, Q., Zhu, J., Han, W., Hu, H., Fang, J. and Xie, Z.: Patterns of plant carbon, nitrogen, and phosphorus concentration in relation to productivity in China's terrestrial ecosystems, Proc. Natl. Acad. Sci. U. S. A., 115(16), 4033–4038, doi:10.1073/pnas.1700295114, 2018b.

Terrer, C., Jackson, R. B., Prentice, I. C., Keenan, T. F., Kaiser, C., Vicca, S., Fisher, J. B., Reich, P. B., Stocker, B. D., Hungate, B. A., Peñuelas, J., McCallum, I., Soudzilovskaia, N. A., Cernusak, L. A., Talhelm, A. F., Van Sundert, K., Piao, S., Newton, P. C. D., Hovenden, M. J., Blumenthal, D. M., Liu, Y. Y., Müller, C., Winter, K., Field, C. B., Viechtbauer, W., Van Lissa, C. J., Hoosbeek, M. R., Watanabe, M., Koike, T., Leshyk, V. O., Polley, H. W. and Franklin, O.: Nitrogen and phosphorus constrain the CO2 fertilization of global plant biomass, Nat. Clim. Chang., 9(9), 684–689, doi:10.1038/s41558-019-0545-2, 2019.

Thornton, P. E., Lamarque, J.-F., Rosenbloom, N. A. and Mahowald, N. M.: Influence of carbon-nitrogen cycle coupling on land model response to CO2 fertilization and climate variability, Glob. Biogeochem. Cycle, 21(4), doi:10.1029/2006GB002868, 2007.

https://doi.org/10.5194/essd-2020-398
Preprint. Discussion started: 8 March 2021

Vincent, A. G., Sundqvist, M. K., Wardle, D. A. and Giesler, R.: Bioavailable soil phosphorus decreases with increasing elevation in a subarctic tundra landscape, PLoS ONE, 9(3), e92942, doi:10.1371/journal.pone.0092942, 2014.

Vitousek, P.: Nutrient cycling and nutrient use efficiency, Am. Nat., 119(4), 553–572, doi:10.1086/283931, 1982.

Vitousek, P. M. and Howarth, R. W.: Nitrogen limitation on land and in the sea: How can it occur?, Biogeochemistry, 13(2), 87–115, doi:10.1007/BF00002772, 1991.

Vitousek, P. M., Porder, S., Houlton, B. Z. and Chadwick, O. A.: Terrestrial phosphorus limitation: mechanisms, implications, and nitrogen—phosphorus interactions, Ecological Applications, 20(1), 5–15, 2010.

Wang, Z., Townsend, P. A., Schweiger, A. K., Couture, J. J., Singh, A., Hobbie, S. E. and Cavender-Bares, J.: Mapping foliar functional traits and their uncertainties across three years in a grassland experiment, Remote Sensing of Environment, 221, 405–416, doi:10.1016/j.rse.2018.11.016, 2019.

Warton, D. I., Duursma, R. A., Falster, D. S. and Taskinen, S.: smatr 3– an R package for estimation and inference about allometric lines, Methods in Ecology and Evolution, 3(2), 257–259, doi:https://doi.org/10.1111/j.2041-210X.2011.00153.x, 2012.

Wieder, W. R., Cleveland, C. C., Smith, W. K. and Todd-Brown, K.: Future productivity and carbon storage limited by terrestrial nutrient availability, Nat. Geosci., 8(6), 441–444, doi:10.1038/ngeo2413, 2015.

Yang, Y.-H., Ma, W.-H., Mohammat, A. and Fang, J.-Y.: Storage, patterns and controls of soil nitrogen in China, Pedosphere, 17(6), 776–785, doi:10.1016/S1002-0160(07)60093-9, 2007.

Zhang, C., Tian, H., Liu, J., Wang, S., Liu, M., Pan, S. and Shi, X.: Pools and distributions of soil phosphorus in China, Glob. Biogeochem. Cycle, 19(1), GB1020, doi:10.1029/2004GB002296, 2005.

Zhang, J., Zhao, N., Liu, C., Yang, H., Li, M., Yu, G., Wilcox, K., Yu, Q. and He, N.: C:N:P stoichiometry in China's forests: From organs to ecosystems, Funct. Ecol., 32(1), 50–60, doi:10.1111/1365-2435.12979, 2018.

https://doi.org/10.5194/essd-2020-398
Preprint. Discussion started: 8 March 2021

Zhang, Y.W., Guo Y.P, Tang Z.Y., Feng Y.H., Zhu X.R., Xu W.T., Bai Y.F., Zhou G.Y., Xie Z.Q., Fang J.Y.: Patterns of nitrogen and phosphorus pools in terrestrial ecosystems in China, Dryad, Dataset, https://datadryad.org/stash/share/78EBjhBqNoam2jOSoO1AXvbZtgIpCTi9eT-eGE7wyOk, 2020.

https://doi.org/10.5194/essd-2020-398
Preprint. Discussion started: 8 March 2021

Table.1. N and P stocks of vegetation, litter, soil and total ecosystem in forest, shrublands and grasslands in China.

Vegetation type group	Vegetation type	Area (10^6 ha)	N pool (10^6 Mg)				P pool (10^6 Mg)			
			Vegetation	Soil	Litter	Ecosystem	Vegetation	Soil	Litter	Ecosystem
Forest	EBF	45.59	13.08	587.48	1.93	608.73	1.89	193.27	0.10	195.26
	DBF	91.14	43.43	665.60	4.25	713.29	8.37	277.61	0.74	286.71
	ENF	99.97	34.93	1074.18	3.58	1112.69	5.59	377.27	0.23	383.08
	DNF	19.79	7.53	84.76	1.73	94.03	4.61	123.33	0.75	128.70
	MF	13.25	6.47	96.95	0.65	104.07	1.38	42.08	0.13	43.59
	subtotal	***269.75***	***111.69***	***2508.98***	***12.14***	***2632.80***	***21.84***	***1013.55***	***1.96***	***1037.34***
Shrubland	EBS	21.65	1.56	160.54	0.61	162.70	0.20	52.95	0.03	53.18
	DBS	63.94	5.30	598.39	1.40	605.09	0.58	220.48	0.09	221.15
	ENS	1.36	0.06	13.29	0.01	13.36	0.008	5.40	0.0006	5.41
	SS	17.35	0.22	48.66	0.21	49.10	0.02	81.85	0.01	81.88
	subtotal	***104.31***	***7.14***	***820.88***	***2.23***	***830.24***	***0.80***	***360.69***	***0.13***	***361.62***
Grassland	ME	59.62	17.87	994.70	0.13	1012.70	1.33	217.20	0.005	218.54
	ST	190.08	36.31	1562.94	0.22	1599.47	2.32	569.27	0.02	571.61
	TU	24.39	2.39	171.02	0.10	173.51	0.26	84.44	0.01	84.71
	SG	139.27	40.78	1376.02	0.09	1416.89	2.33	1576.48	0.02	1578.83
	subtotal	***413.35***	***97.35***	***4104.68***	***0.55***	***4202.58***	***6.24***	***2447.41***	***0.05***	***2453.70***
Total		***787.4***	***216.17***	***7434.53***	***14.92***	***7665.62***	***28.88***	***3821.64***	***2.14***	***3852.66***

EBF, evergreen broadleaf forest; DBF, deciduous broadleaf forest; ENF, evergreen needle-leaf forest; DNF, deciduous needle-leaf forest; MF, broadleaf and needle-leaf forest; EBS, evergreen broadleaf shrub; DBS, deciduous broadleaf shrub; ENS, evergreen needle-leaf shrub; SS, sparse shrub; ME, meadow; ST, steppe; TU, tussock; and SG, sparse grassland.

https://doi.org/10.5194/essd-2020-398
Preprint. Discussion started: 8 March 2021

Table.2. N and P stocks of plant organs (leaf, stem and root) in forest, shrublands and grasslands in China.

Vegetation type group	Vegetation type	Area (10^6 ha)	N pool (10^6 Mg)			P pool (10^6 Mg)		
			Leaf	Stem	Root	Leaf	Stem	Root
Forest	EBF	45.59	3.849	10.863	4.614	0.273	1.308	0.313
	DBF	91.14	6.820	23.289	13.322	0.555	4.680	3.133
	ENF	99.97	10.185	17.090	7.653	1.256	3.205	1.125
	DNF	19.79	1.661	4.336	1.535	0.292	3.691	0.631
	MF	13.25	1.326	3.714	1.428	0.117	0.931	0.328
	subtotal	***269.75***	***23.841***	***59.293***	***28.552***	***2.493***	***13.814***	***5.531***
Shrubland	EBS	21.65	0.632	0.051	0.872	0.045	0.074	0.083
	DBS	63.94	1.682	0.205	3.413	0.124	0.164	0.290
	ENS	1.36	0.037	0.001	0.022	0.005	0.0001	0.003
	SS	17.35	0.070	0.021	0.129	0.005	0.005	0.006
	subtotal	***104.31***	***2.420***	***0.279***	***4.436***	***0.179***	***0.243***	***0.382***
Grassland	ME	59.62	1.181	0	16.687	0.121	0	1.213
	ST	190.08	2.818	0	33.492	0.261	0	2.055
	TU	24.39	0.559	0	1.830	0.058	0	0.201
	SG	139.27	1.573	0	39.211	0.244	0	2.084
	subtotal	***413.35***	***6.132***	***0***	***91.220***	***0.685***	***0***	***5.553***
Total		***787.4***	***32.394***	***59.571***	***124.209***	***3.357***	***14.057***	***11.466***

See table 1 for abbreviations.

https://doi.org/10.5194/essd-2020-398
Preprint. Discussion started: 8 March 2021

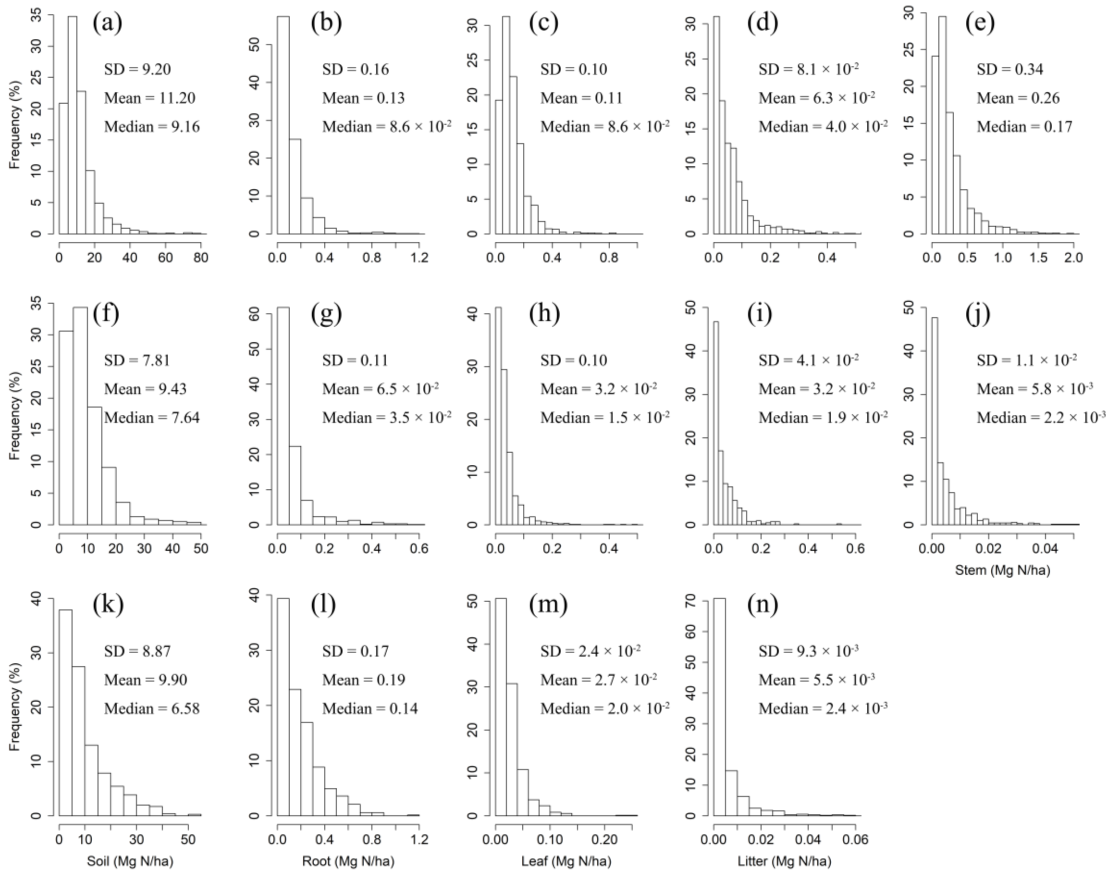

Fig. 1. Frequency distributions of N densities in soil, roots, leaves, litter and woody stems in forests (a–e), shrublands (f–j) and grasslands (k–n) in China.

https://doi.org/10.5194/essd-2020-398
Preprint. Discussion started: 8 March 2021

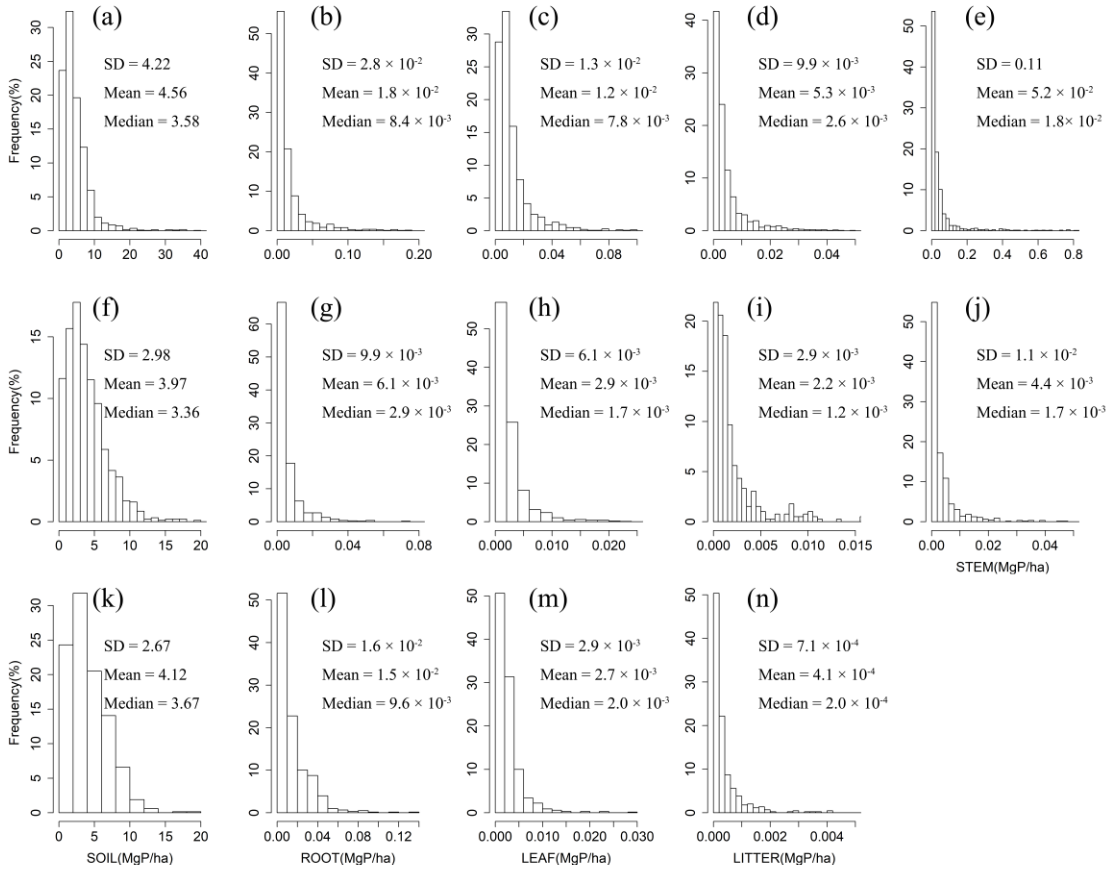

Fig. 2. Frequency distributions of P densities in soil, roots, leaves, litter and woody stems in forests (a–e), shrublands (f–j) and grasslands (k–n) in China.

https://doi.org/10.5194/essd-2020-398
Preprint. Discussion started: 8 March 2021

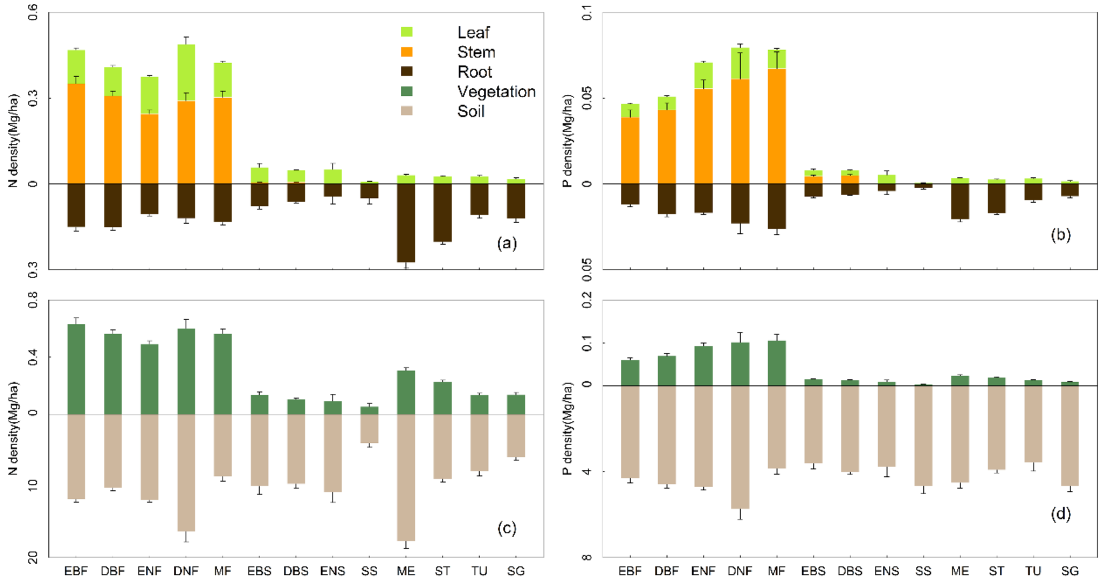

Fig. 3. N and P density allocations among leaf, stem and root (a & b) and between vegetation and soil (c & d) in 13 Vegetation types. See table 1 for abbreviations. The error bar represents standard error. Notice that the y axes above and below zero are disproportionate.

https://doi.org/10.5194/essd-2020-398
Preprint. Discussion started: 8 March 2021

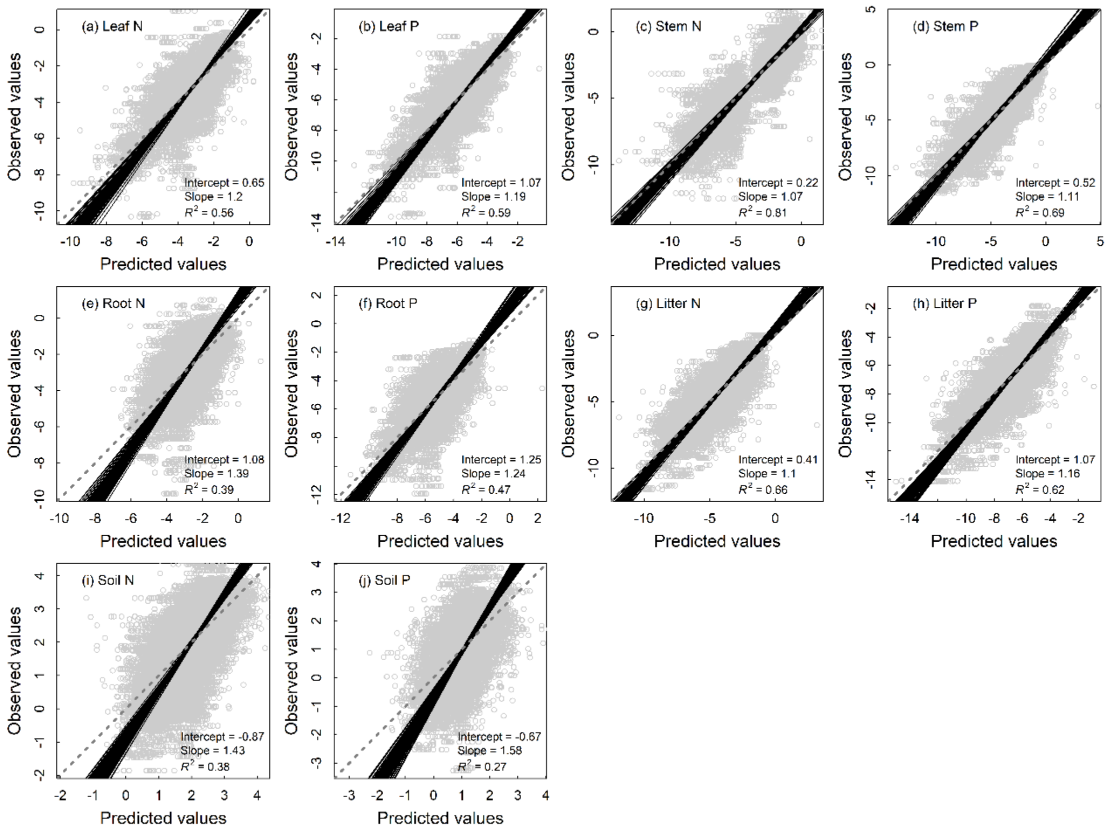

Fig. 4. Fitting performance of artificial neural network models for different components of terrestrial ecosystems in China based on 100 times of replications with the 10% validation data. Solid lines represent all the fitting lines by standard major axis regression, and the displayed parameters stand for the average conditions. The dashed line denotes the 1:1 line.

https://doi.org/10.5194/essd-2020-398
Preprint. Discussion started: 8 March 2021

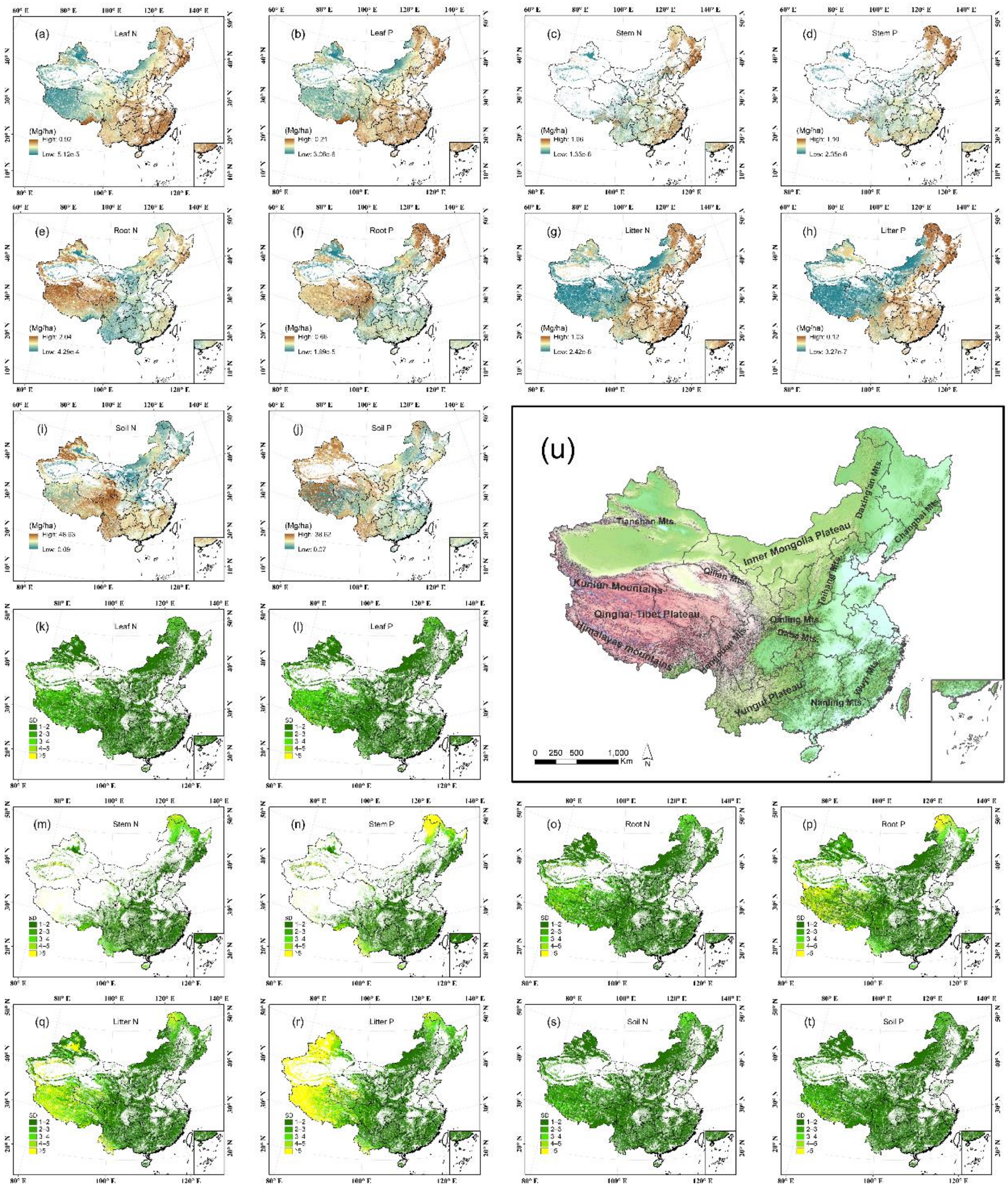

Fig. 5. Predicted spatial patterns of N and P densities with a resolution of 1 km (a–j) and their prediction standard deviations (SDs) (k–t) in each component of terrestrial ecosystems in China based on 100 replications. The topographic map of China (u) is also shown.

https://doi.org/10.5194/essd-2020-398
Preprint. Discussion started: 8 March 2021

Earth System Science Data
Open Access
Discussions

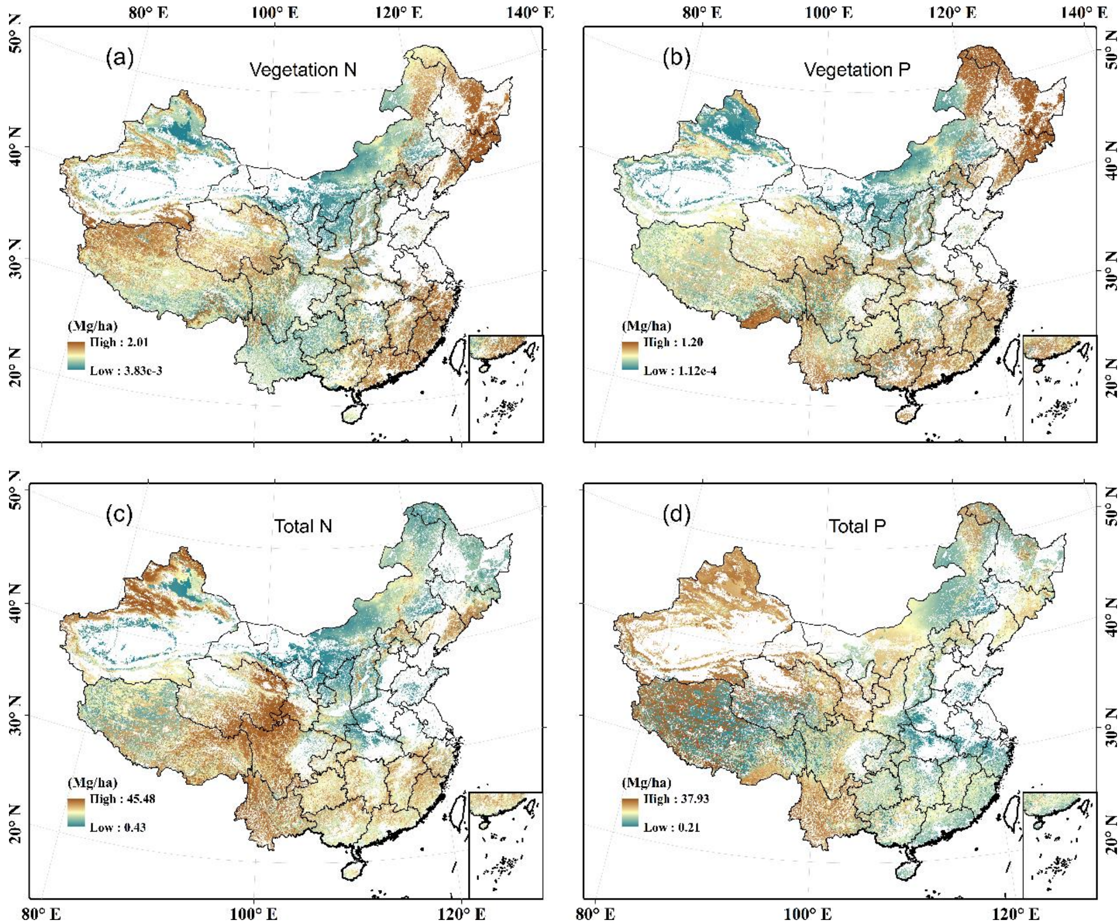

Fig. 6. Spatial patterns of N and P densities with a resolution of 1 km in vegetation (a & b, the sum of leaves, stems and roots) and ecosystems (c and d, the sum of leaves, stems, roots, litter and soil) of terrestrial ecosystems in China.